Thermochimica Acta, 115 (1987) 11–19
Elsevier Science Publishers B.V., Amsterdam – Printed in The Netherlands

HEAT CAPACITY OF $2Al_4C_3 \cdot SiC$ FROM 447 TO 1447 K AND ENTHALPY OF PERITECTIC DECOMPOSITION OF Al_4C_3, $2Al_4C_3 \cdot SiC$, AND $Al_4C_3 \cdot SiC$

L.L. ODEN and R.P. BEYER

Albany Research Center, Bureau of Mines, U.S. Department of the Interior, P.O. Box 70, Albany, OR 97321 (U.S.A.)

(Received 28 July 1986; in final form 23 October 1986)

ABSTRACT

The molar heat capacity of $2Al_4C_3 \cdot SiC$ and the enthalpy of peritectic decomposition of Al_4C_3, $2Al_4C_3 \cdot SiC$, and $Al_4C_3 \cdot SiC$ were measured by the Bureau of Mines to provide fundamental data to assist in the development of a carbothermic reduction process for aluminum. The molar heat capacity of $2Al_4C_3 \cdot SiC$ was measured by differential scanning calorimetry from 447 to 1447 K. The enthalpy of peritectic decomposition was calculated from time–temperature thermal analyses of samples, synthetic sapphire (NBS Standard Reference Material 720), and an empty crucible.

The value at $T = 298.15$ K for $C^0_{p,m}$ of $2Al_4C_3 \cdot SiC$ is 260.24 J K^{-1} mol^{-1}. The enthalpy of peritectic decomposition for Al_4C_3 at 2429 K is (140 ± 20) kJ mol^{-1}, for $2Al_4C_3 \cdot SiC$ starting at 2358 K it is (210 ± 50) kJ mol^{-1}, and for $Al_4C_3 \cdot SiC$ starting at 2345 K it is (160 ± 20) kJ mol^{-1}.

INTRODUCTION

One goal of the Bureau of Mines is to provide thermodynamic quantities for minerals and related inorganic compounds, particularly as related to critical and/or strategic materials such as aluminum. As part of this effort, the molar heat capacity of $2Al_4C_3 \cdot SiC$ and the enthalpy of peritectic decomposition of Al_4C_3, $2Al_4C_3 \cdot SiC$, and $Al_4C_3 \cdot SiC$ were determined. The intermediate phases $2Al_4C_3 \cdot SiC$, as identified in this laboratory and reported by Kidwell et al. [1], and $Al_4C_3 \cdot SiC$, as reported by Barczak [2] and confirmed in this work, are the only ternary phases in the Al–Si–C system [3]. The molar heat capacity was measured with a differential scanning calorimeter (DSC) over the range 447–1447 K. The decomposition enthalpies were measured in a graphite resistance furnace by time–temperature thermal analysis. No report of measurements of these thermodynamic quantities was found in the literature.

EXPERIMENTAL

Samples to be analyzed were prepared by reacting the high-purity elements (spectrographic-grade graphite, 99.99 mass% Al, and 99.999 mass% Si) in α-Al_2O_3 crucibles at 1770 K for 2 h, grinding and mixing the partially reacted mixture, reheating to 1870 K for 2 h in graphite crucibles, grinding and mixing, then reheating to 2270 K for 2 h in graphite crucibles. A positive pressure (135 kPa) of high-purity argon (99.995 vol%) was maintained in the furnace during each of the preparative heat treatments. A running mass balance throughout the preparation process indicated that 102% of the stoichiometric Al was required in the initial mixture of elements to compensate for vaporization losses. Vaporization of silicon was not significant. X-ray diffraction analysis identified the phases present after each step. The final products were single-phase except for Al_4C_3, which contained an estimated 0.05 weight% graphite.

The molar heat capacities were measured with a model TA2000C simultaneous DSC and thermogravimetric analyzer manufactured by Mettler Instrument Corporation *. The DSC was interfaced with a DEC LSI-11/2 computer through A–D converter and digital input–output cards. This instrument is a heat-flux-type DSC with a sensitivity of approximately 1.0 $\mu V\ mW^{-1}$ and a nominal accuracy of $\pm$ 5%. Two separate series of measurements were made (I and II). For each series, three determinations were made with (1) an empty capsule, (2) a capsule filled with synthetic sapphire, and (3) a capsule filled with $2Al_4C_3 \cdot SiC$. For series I, 0.1244 g of $2Al_4C_3 \cdot SiC$ was used with a 0.4701-g platinum capsule. For series II, 0.0744 g of $2Al_4C_3 \cdot SiC$ was used with a 0.4813-g platinum capsule. For all the determinations, the capsule was placed into the DSC, which was then evacuated and filled with argon. The DSC was operated at a scan rate of 0.167 $K\ s^{-1}$ in 50-K steps from 422 to 1472 K. The results were analyzed according to the "enthalpy method", as described by Mraw and Naas [4].

Molar heats of peritectic decomposition for the carbides were determined by time–temperature thermal analysis of the samples, synthetic sapphire reference material, and empty crucibles in a resistance furnace having a 5-cm diameter by 20-cm long graphite element and programmable power supply. Heating and cooling rates could be varied over the range 0.08–8 $K\ s^{-1}$ in either high vacuum or an inert atmosphere. A positive pressure (135 kPa) of high-purity argon was used throughout this investigation. Samples were analyzed in 10-mm diameter by 20-mm high graphite crucibles with 0.8-mm walls containing a central graphite sight hole 4 mm in diameter by 20 mm long with 0.4-mm walls. A typical crucible, lid, and sight hole

* Reference to specific manufacturers or products does not imply endorsement by the Bureau of Mines.

weighing about 1 g contained about 0.8 g of sample. Supergraph 710 grade graphite, a very dense, fine-grained material from Aremco Products Inc., was used for crucible, lid, and sight hole. The reference material, synthetic sapphire, was analyzed in Nb crucibles 10 mm in diameter by 16 mm high with 0.25-mm walls. Ends for the crucibles were deep-drawn from 0.08-mm thick Ta foil. A closed-end, 4-mm diameter by 18-mm high Nb tube with 0.08-mm walls formed the sight hole. A typical Ta–Nb crucible weighing 1.3 g contained about 1.9 g of synthetic sapphire.

The sample crucible was heated within a larger graphite canister 45 mm in diameter by 115 mm long with 4-mm walls that was insulated top and bottom with graphite felt. The upper insulation contained a 6-mm diameter hole for sighting upon the sample crucible.

Temperatures were determined at heating and cooling rates of 0.17 K s^{-1} by optical pyrometry using an automatic indicating brightness instrument (PYROPHOTO II) from the Pyrometer Instrument Company and a Bascom Turner electronic recorder. The pyrometer indicated temperature continuously in three ranges from 1075 to 2575 K with an uncertainty varying from $\pm 1°$ at 1075 K to $\pm 2.5°$ at 2575 K. The recorder digitized the analog signals from the pyrometer and stored the data, which were later transferred to a Hewlett-Packard 2647A computer. The data were then smoothed using a digital filter and plotted on a Hewlett-Packard 9872A recorder with a 3-fold scale expansion. The area was determined by graphical integration.

RESULTS

The experimental molar heat capacities are listed chronologically in Table 1. The uncertainties of the DSC measurements were determined by measuring the heat capacity of MgO in two separate series and comparing the measured values with accepted values from Pankratz [5]. The uncertainties were found to vary from 4.5% at 500 K to 2.7% at 1450 K.

The molar heat capacities were smoothed using a curve-fitting routine developed by Justice [6] to give the values of $C^0_{p,m}$; $\{S^0_m(T) - S^0_m(298.15\ K)\}$; $-\{G^0_m(T) - H^0_m(298.15\ K)\}/T$; and $\{H^0_m(T) - H^0_m(298.15\ K)\}$, listed in Table 2. The heat capacities were extrapolated to 298.15 K and from 1100 to 1500 K by using the sum of $2C^0_{p,m}(Al_4C_3) + C^0_{p,m}(SiC)$. Heat capacity values for SiC are from Humphrey et al. [7] and Chekhovskoy [8] and for Al_4C_3 from Furukawa et al. [9] and Binford et al. [10]. Data above 1100 K were not used in the final fit due to reaction of the sample with the platinum crucible. The molar heat capacity curve is shown in Fig. 1. The molar heat capacity curve for MgO is shown in Fig. 2.

The observed time–temperature thermal analysis curves for synthetic sapphire and the three Al–C and Al–Si–C compounds are shown in Fig. 3.

TABLE 1

Experimental molar heat capacities of $2Al_4C_3 \cdot SiC$ by differential scanning calorimetry

T (K)	$C^0_{p,m}$ ($J\,K^{-1}\,mol^{-1}$)	T (K)	$C^0_{p,m}$ ($J\,K^{-1}\,mol^{-1}$)	T (K)	$C^0_{p,m}$ ($J\,K^{-1}\,mol^{-1}$)
		1097	410.6	747	380.8
Series I		1147	417.7	797	384.8
		1197	416.8	847	392.8
447	325.6	1247	419.6	897	394.5
497	337.5	1297	419.8	947	398.2
547	350.0	1347	419.0	997	404.8
597	359.7	1397	419.2	1047	412.1
647	366.9	1447	417.5	1097	417.3
697	375.9			1147	421.8
747	383.4	*Series II*		1197	427.7
797	387.9			1247	431.6
847	392.9	497	341.2	1297	435.1
897	397.9	547	343.7	1347	435.8
947	400.7	597	356.8	1397	429.8
997	403.3	647	368.6	1447	417.9
1047	408.9	697	373.6		

The equation describing the events in the thermal analyzer was assumed to be

$$\frac{d}{dt}(MC_pT) = U(T_2 - T_1) + \frac{dH}{dt} \tag{1}$$

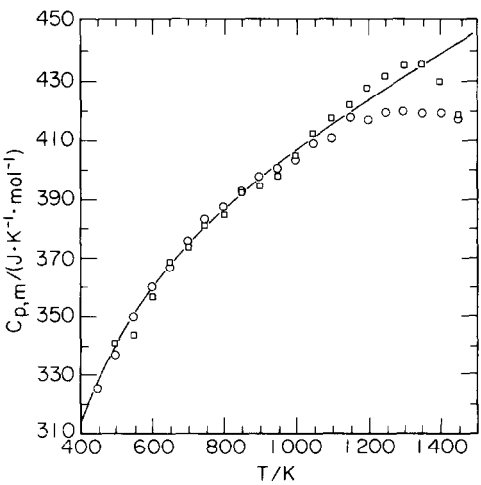

Fig. 1. Heat capacities of $2Al_4C_3 \cdot SiC$. (○) Series I; (□) series II; (———) $2C^0_{p,m}(Al_4C_3) + C^0_{p,m}(SiC)$ from Pankratz [5].

TABLE 2

Molar thermodynamic properties of $2Al_4C_3 \cdot SiC$ (values below 450 K and above 1200 K are extrapolated)

T (K)	$C^0_{p,m}$ (J K^{-1} mol^{-1})	$S^0_m(T) - S^0_m$(298.15) (J K^{-1} mol^{-1})	$-\{G^0_m(T) - H^0_m$(298.15)$\}/T$ (J K^{-1} mol^{-1})	$H^0_m(T) - H^0_m$(298.15) (kJ mol^{-1})
298.15	260.236	0.0	0.0	0.0
300	261.431	1.613	0.005	0.483
350	288.977	44.090	3.296	14.278
400	309.726	84.092	10.922	29.268
450	325.984	121.547	21.156	45.176
500	339.132	156.596	32.967	61.815
550	350.050	189.446	45.715	79.052
600	359.324	220.312	58.992	96.792
650	367.362	249.398	72.531	114.964
700	374.452	276.887	86.155	133.513
750	380.807	302.942	99.746	152.397
800	386.587	327.706	113.226	171.584
850	391.913	351.305	126.542	191.048
900	396.882	373.848	139.660	210.769
950	401.556	395.433	152.558	230.732
1000	406.028	416.145	165.223	250.922
1100	414.465	455.243	189.833	291.951
1200	422.486	491.653	213.485	333.801
1300	430.294	525.779	236.208	376.441
1400	438.035	557.950	258.052	419.858
1500	445.813	588.436	279.070	464.050

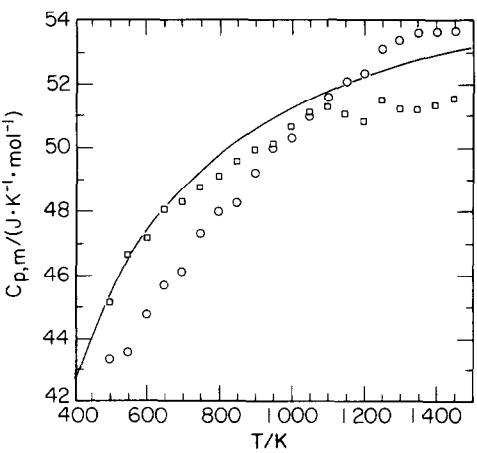

Fig. 2. Heat capacity of MgO. (○) Series I; (□) series II; (———) $C^0_{p,m}$(MgO) from Pankratz [5].

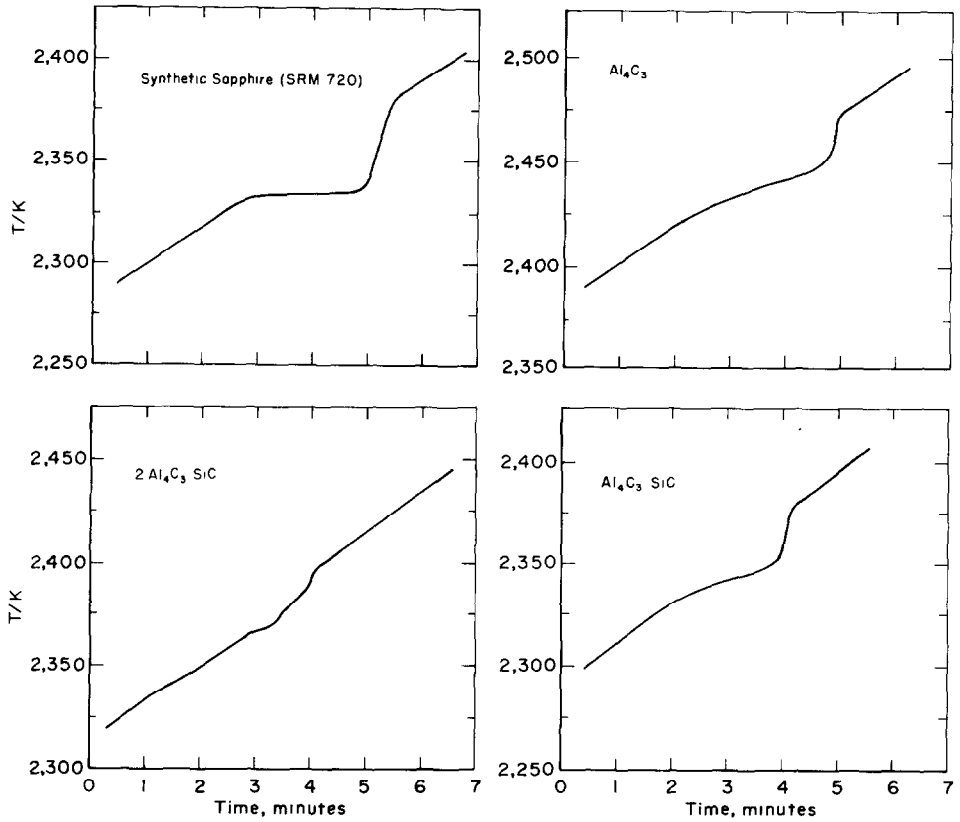

Fig. 3. Time–temperature plots for synthetic sapphire, Al_4C_3, $2Al_4C_3 \cdot SiC$, and $Al_4C_3 \cdot SiC$.

where M is the sample mass, C_p is the sample heat capacity, T_1 is the temperature of the sample, U is a temperature-dependent heat transfer coefficient, T_2 is the furnace temperature, and H is any transition enthalpy.

During a period of transition, as in melting or peritectic decomposition, $dT/dt = 0$ and eqn. (1) becomes

$$\int dH = -\int_{t_1}^{t_2} U(T_2 - T_1)dt \tag{2}$$

In the present case, the integral on the right-hand side of eqn. (2) was taken to be the shaded area shown in Fig. 4. These areas were calculated for all the compounds measured, and the transition enthalpy, ΔH, for each was calculated by a simple ratio with the enthalpy of fusion of synthetic sapphire, $\Delta H(Al_2O_3)$, as follows:

$$\Delta H = \Delta H(Al_2O_3) \cdot A/A(Al_2O_3) \cdot M/M(Al_2O_3) \cdot W/W(Al_2O_3) \tag{3}$$

where A, M, and W are area, mass, and molecular weight, respectively. In this way, the variable U from eqn. (2) cancels.

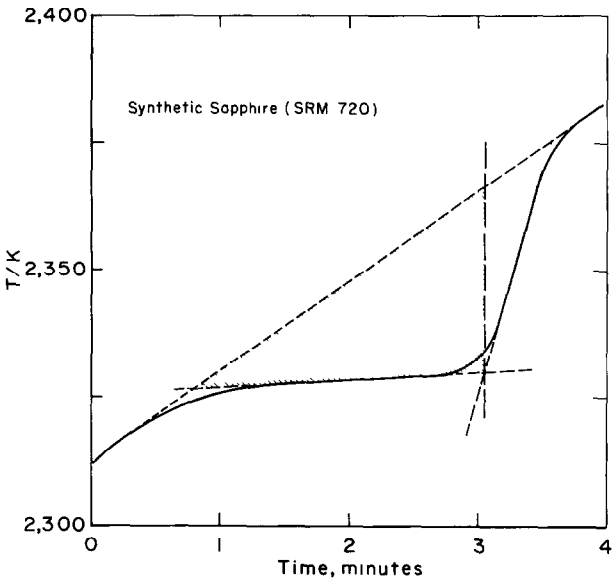

Fig. 4. Estimation of decomposition enthalpy area from the time–temperature plots.

To determine if the value for U was dependent upon the emissivity of the crucible, synthetic sapphire was measured in a Ta–Nb crucible, and the measurement was repeated with the same crucible inside a graphite crucible. Identical time–temperature plots were observed. Repeated measurements on sapphire gave an overall uncertainty for ΔH of $\pm$ 10%. The measured values and the experimental uncertainties for Al_4C_3, $2Al_4C_3 \cdot SiC$, and $Al_4C_3 \cdot SiC$ are (140 $\pm$ 20), (210 $\pm$ 50), and (160 $\pm$ 20) kJ mol^{-1}, respectively.

DISCUSSION

The Al–C and Al–Si–C compounds decompose on heating by binary peritectic, ternary peritectic, and quasibinary peritectic reactions described by eqns. (4), (5), and (6), respectively [3], where liquid (l) and solid (s) compositions are represented by simple formulas.

$$Al_4C_3(s) \rightarrow 4AlC_{0.24}(l) + 2.04C(s) \quad (4)$$

$$2Al_4C_3 \cdot SiC(s) \rightarrow 4.72(AlSi_{0.17}C_{0.18})(l) + 3.28(AlSi_{0.06}C_{0.80})(s) + 3.52C(s) \quad (5)$$

$$Al_4C_3 \cdot SiC(s) \rightarrow 4(AlSi_{0.25}C_{0.20})(l) + 3.20C(s) \quad (6)$$

The atom fraction of compound that melts at the peritectic temperature is readily calculated to be 0.71, 0.40, and 0.64 for Al_4C_3, $2Al_4C_3 \cdot SiC$, and $Al_4C_3 \cdot SiC$, respectively. Expressed as weight fractions, the values become 0.87, 0.49, and 0.79. The significance of these values is that the magnitude of

the observed thermal arrest for a given quantity of material is related to the fraction of material that melts, and therefore the thermal arrest per unit mass of material is expected to be smallest for $2Al_4C_3 \cdot SiC$, larger for $Al_4C_3 \cdot SiC$, and largest for Al_4C_3.

The thermal arrest for $2Al_4C_3 \cdot SiC$ is not only smallest, but is also atypical in shape owing to a complex series of reactions that occur prior to and after the peritectic decomposition [3]. These reactions are initiated by the vaporization of Al during the analysis, resulting in the formation of $Al_4C_3 \cdot SiC$ by eqn. (7):

$$2Al_4C_3 \cdot SiC(s) \rightarrow 4Al(gas) + 3C(s) + Al_4C_3 \cdot SiC(s) \quad (7)$$

The experimental weight loss for a sample of $2Al_4C_3 \cdot SiC$ initially weighing 0.8242 g was 0.0210 g. Assuming that half of the weight loss occurred by vaporization of Al during heating, then up to 0.0319 g, or 3.8%, of the sample may have decomposed by eqn. (7). A quasiperitectic reaction occurs on heating at 2338 K (eqn. 8), by which 0.0285 g, or 3.6%, of the sample would be involved:

$$2Al_4C_3 \cdot SiC(s) + 3.0(Al_4C_3 \cdot SiC)(s) \rightarrow 20.0(AlSi_{0.20}C_{0.18})(l) + 15.4C(s) \quad (8)$$

The result of the quasiperitectic reaction, eqn. (8), is a deviation from linearity of the time–temperature curve beginning at about 2338 K. Ternary peritectic decomposition of the remaining $2Al_4C_3 \cdot SiC$ ($\sim$ 96% of the initial sample) then occurs at 2358 K (eqn. 5). The solid produced by eqn. (5) then continues to decompose to liquid and carbon up to about 2363 K, where the sample is then carbon and a liquid Al–Si alloy containing 13.5 atom% C.

For purposes of calculating the enthalpy of decomposition for $2Al_4C_3 \cdot SiC$, the area was considered beginning at the first deviation from linearity (2338 K) and extending through the near-isothermal region beginning at 2358 K.

A similar but less complicated sequence of reactions also occurs for $Al_4C_3 \cdot SiC$, which partially decomposes to aluminum vapor and SiC on heating. The resulting SiC reacts at 2345 K with $Al_4C_3 \cdot SiC$ in a quasiperitectic reaction (eqn. 9):

$$Al_4C_3 \cdot SiC(s) + 0.49SiC(s) \rightarrow 4AlSi_{0.37}C_{0.15}(l) + 3.9C(s) \quad (9)$$

The remaining $Al_4C_3 \cdot SiC$ undergoes complete decomposition by quasibinary peritectic reaction (eqn. 6) at 2363 K. The result of eqn. (9) is a deviation from linearity of the time–temperature curve beginning at 2345 K. The decomposition of $Al_4C_3 \cdot SiC$ is complete by 2363 K.

SUMMARY AND CONCLUSIONS

This research has demonstrated that time–temperature thermal analysis can provide useful enthalpies for reactions occurring at high temperatures.

The heat capacity of $2Al_4C_3 \cdot SiC$ determined in this work, the heat capacity of $Al_4C_3 \cdot SiC$ reported previously by Beyer and Johnson [11], and the enthalpy of peritectic decomposition of Al_4C_3, $2Al_4C_3 \cdot SiC$, and $Al_4C_3 \cdot SiC$ complete the determination of the thermodynamic properties planned for the compounds in the Al–Si–C system. These data are useful for mathematical modeling of carbothermic reduction processes using abundant domestic aluminous raw materials such as clays, oil shale retorting residues, and fly ash from coal-fired power plants.

REFERENCES

1 B.L. Kidwell, L.L. Oden and R.A. McCune, J. Appl. Crystallogr., 17 (1984) 481.
2 V.J. Barczak, J. Am. Ceram. Soc., 44 (1961) 299.
3 L.L. Oden and R.A. McCune, Metall. Trans. A, submitted.
4 S.C. Mraw and D.F. Naas, J. Chem. Thermodyn., 11 (1979) 507.
5 L.B. Pankratz, U.S. Bur. Mines Bull. 672 (1982).
6 B.H. Justice, FITAB Program, Univ. Mich., Ann Arbor, MI, COO-1149-143, 1969.
7 G.L. Humphrey, S.S. Todd, J.P. Coughlin and E.G. King, U.S. Bur. Mines Rep. Invest. 4888 (1952).
8 V.Y. Chekhovskoy, J. Chem. Thermodyn., 3 (1971) 289.
9 G.T. Furukawa, T.G. Douglas, W.G. Saba and A.C. Victor, J. Res. Natl. Bur. Stand., Sect. A, 69 (1965) 423.
10 J.S. Binford, J.M. Strohmenger and T.H. Herbert, J. Phys. Chem., 71 (1967) 2404.
11 R.P. Beyer and E.A. Johnson, J. Chem. Thermodyn., 16 (1984) 1025.